Volume 10
Number 3
March 2023
Pages 697–950

Environmental Science Nano

rsc.li/es-nano

ISSN 2051-8153

ROYAL SOCIETY OF CHEMISTRY

PAPER
Mohammed Baalousha *et al.*
Urban runoff drives titanium dioxide engineered particle concentrations in urban watersheds: field measurements

Environmental Science Nano

ROYAL SOCIETY OF CHEMISTRY

PAPER

Cite this: *Environ. Sci.: Nano*, 2023, **10**, 718

Urban runoff drives titanium dioxide engineered particle concentrations in urban watersheds: field measurements†

Md Mahmudun Nabi,[a] Jingjing Wang,[a] Mahdi Erfani,[b] Erfan Goharian[b] and Mohammed Baalousha *[a]

Received 6th September 2022,
Accepted 21st December 2022

DOI: 10.1039/d2en00826b

rsc.li/es-nano

Urban runoff is a significant source of pollutants, including incidental and engineered nanoparticles, to receiving surface waters. The aim of this study is to investigate the impact of urbanization on the concentrations of TiO_2 engineered particles in urban surface waters. The study area boundaries are limited to the Lower Saluda and Nicholas Creek-Broad River from upstream, and outlet of upper Congaree River in Columbia, South Carolina, United States from downstream. This sampling area captures a significant footprint of the urban area of the city of Columbia. Water samples were collected daily from four sites during two rain events. All samples were analyzed for total metal concentrations following acid digestion and for particle number concentration and elemental composition using single particle-inductively coupled plasma-time of flight-mass spectrometry (SP-ICP-TOF-MS). The Ti/Nb ratios in the Broad and Congaree River samples are generally higher than those of natural background ratios, indicating contamination of these two rivers with anthropogenic Ti-bearing particles. Clustering of multi-metal nanoparticles (mmNPs) demonstrated that Ti-bearing particles are distributed mainly among three clusters, FeTiMn, AlSiFe, and TiMnFe, which are typical of naturally occurring iron oxide, clay, and titanium oxide particles, indicating the absence of significant number of anthropogenic multi-element Ti-bearing particles. Thus, anthropogenic Ti-bearing particles are attributed to single-metal particles; that is pure TiO_2 particles. The total concentration of anthropogenic TiO_2 in the rivers was determined by mass balance calculation using bulk titanium concentration and increases in Ti/Nb above the natural background ratio. The concentration of anthropogenic TiO_2 increases following the order 0 to 24 μg L^{-1} in the Lower Saluda River <0 to 663 μg L^{-1} in the Broad River <43 to 1051 μg L^{-1} in Congaree River at Cayce <58 to 5050 μg L^{-1} in the Congaree River at Columbia. The concentration of anthropogenic TiO_2 increases with increases in urban runoff. The source of anthropogenic TiO_2 is attributed to diffuse urban runoff. This study demonstrates that diffuse urban runoff results in high concentrations of TiO_2 particles in urban surface waters during and following rainfall events which may pose increased risks to aquatic organisms during these episodic events.

Environmental significance

Spatiotemporal monitoring of anthropogenic (engineered and incidental) metal-bearing nanoparticles in environmental systems is essential to improve the understanding of the nature, sources, magnitude of exposure, environmental fate, and risk assessment of these materials. Here we monitored – daily over 16 days – the concentrations of anthropogenic Ti-bearing particles in three rivers (Lower Saluda, Broad, and Congaree) within the urban outskirts of the city of Columbia, South Carolina, United States. The higher bulk Ti/Nb mass ratios than the natural background ratios and the similarity of natural the fingerprint of multi-element Ti-bearing to those of natural particles suggest that the samples are contaminated with single metal Ti-bearing particles which can be attributed to pure TiO_2 particles. The concentration of anthropogenic TiO_2 were minimal in the Lower Saluda River downstream Lake Murray reservoir and increased from the Broad to the Congaree River along the city of Columbia. The concentration of anthropogenic TiO_2 followed the same trend of increases and decreases as the discharge/runoff. Thus, anthropogenic TiO_2 particles were attributed to urban runoff from the city of Columbia. These findings suggest that aquatic organisms in urban waters within the outskirts and downstream of highly urbanized and mega cities are frequently exposed to transient high concentrations of anthropogenic TiO_2 particles, as well as other particles and contaminants carried with urban runoff.

[a] *Center for Environmental Nanoscience and Risk, Department of Environmental Health Sciences, Arnold School of Public Health, University of South Carolina, SC 29208, USA. E-mail: mbaalous@mailbox.sc.edu*
[b] *Department of Civil and Environmental Engineering, University of South Carolina, SC 29208, USA*

† Electronic supplementary information (ESI) available. See DOI: https://doi.org/10.1039/d2en00826b

1. Introduction

Urban runoff is widely recognized as a major vector of pollutants, including engineered and incidental nanoparticles (ENPs and INPs), from the urban environment to receiving surface waters, contributing to the deterioration of urban surface water quality.[1] Yet, there is a limited understanding of the impacts of urbanization and urban runoff on the concentrations of engineered particles in urban surface waters.[2] Titanium dioxide (TiO_2) is the most widely used engineered particles in the urban environment both as pigments (*e.g.*, 100–300 nm) in paint and as nanosized particles (*e.g.*, 1–100 nm) in self-cleaning surfaces such as photocatalysts.[3] For instance, an estimated 5.3 billion liters per year of paint were used in the United States in 2019, 33% of which (*e.g.*, 1.77 billion liters per year) was used for exterior paint.[4] These uses of TiO_2 result in their release due to wear and tear into the atmosphere and deposition on urban surfaces.[5–9] Rainfall washes the atmospheric deposited particles and carries them into receiving waterbodies. Thus, TiO_2 engineered particles are expected to occur at high concentrations in urban surface waters.

Urban waters receive large amounts of pollution, including TiO_2 engineered particles, from a variety of sources such as industrial discharges, mobile sources (*e.g.*, cars and trucks), residential and commercial wastewater, and polluted stormwater runoff from urban landscape. Recent studies reported high concentrations of TiO_2 engineered particles in road dust (*e.g.*, 0.4–2.5 g kg^{-1}),[10–16] bridge runoff (*e.g.*, 5–150 μg L^{-1}),[17–19] sanitary sewer overflow – impacted surface waters (*e.g.*, 1–100 μg L^{-1}),[20,21] urban runoff – impacted surface waters (*e.g.*, 20 to 140 μg L^{-1}),[22] and industrial discharge – impacted surface waters (*e.g.*, 133 to 266 μg L^{-1}).[23,24] Additionally, a recent modeling study predicted even higher concentrations TiO_2 ENPs (*e.g.*, 619 to 1490 μg L^{-1}) in urban rivers following rainfalls.[25] However, other studies reported much lower concentrations of TiO_2 engineered particles in surface waters released from sunscreens (*e.g.*, 1.5–42.5 μg L^{-1}).[26–30] These discrepancies in the reported TiO_2 engineered particle concentrations can be ascribed to differences in sampling areas, the targeted source of TiO_2 engineered particles, and/or methodological differences.[2]

Monitoring engineered particle concentrations in the environment is challenging because of the similarities of physicochemical properties – such as composition, size, and shape – and the lower abundance of engineered particles compared to naturally occurring counterparts.[31,32] For instance, Ti is the ninth most abundant element in the Earth's crust and is mainly found in minerals such as rutile, ilmenite, sphene, and/or opaque heavy minerals (*e.g.*, titanomagnetite, magnetite, and ilmenite).[33] These minerals always contain trace concentrations of other elements such as Nb, Ta, Sn, Sb, W, V, Cr, Mo, and rare earth elements (REEs).[34,35] These natural elemental impurities are typically removed from the natural Ti-bearing minerals during the manufacturing of TiO_2 engineered particles.[20] Thus, the introduction of TiO_2 engineered particles into environmental systems results in increases in the elemental ratios of Ti to those elements naturally occurring in Ti-bearing minerals (*e.g.*, Ti/Nb,[20,22,36,37] Ti/Al,[27] Ti/REEs,[27] and Ti/V (ref. 23)), which have been used to estimate the concentration TiO_2 engineered particles in environmental systems.

Multi element-single particle analysis by single particle-inductively coupled plasma-time of flight-mass spectrometer (SP-ICP-TOF-MS) is a promising technique in the nanometrology toolbox that has been implemented to differentiate ENPs from NNPs based on the subtle differences in their elemental composition.[20,38] The premise of ICP-TOF-MS is that it detects and quantifies all elements within a single particle at low/trace concentrations, and thus, SP-ICP-TOF-MS is the only method that could be implemented to differentiate ENPs from NNPs in environmental systems at the single particle level. However, the ability of the SP-ICP-TOF-MS to "unequivocally" differentiate ENPs from NNPs based on differences in elemental composition at the single particle level is challenged by the minimal detectable element mass (MDM), which is element dependent.[39,40] The MDM that can be attained by SP-ICP-MS depends on the instrument or elemental sensitivity and the background levels that result from both dissolved analyte and instrumental noise (electronic noise and interferences to the monitored isotope).[40]

The overarching aim of this study is to evaluate the impact of urbanization on the concentrations of TiO_2 engineered particles in urban surface waters. To this end, we collected spatiotemporally resolved water samples from three Rivers within the urban zone of the city of Columbia, South Carolina, United States. We then characterized these water samples for total elemental concentrations using ICP-TOF-MS, estimated the concentrations of anthropogenic TiO_2 engineered particles using mass balance calculations and shifts in elemental ratios above the natural background ratios, and determined particle elemental composition at the single particle level using SP-ICP-TOF-MS.

2. Materials and methods

2.1. Study area

The confluence of the Lower Saluda and Broad Rivers forming the Congaree River at Columbia, South Carolina was selected as the study area to investigate the impact of urbanization on the concentrations of TiO_2 engineered particles in urban surface waters (Fig. 1). Water samples were collected between 27/4/2020 and 12/5/2020 from four locations within the limits of Columbia, South Carolina, United States, including the Lower Saluda River and the Broad River upstream of their confluence, and from Congaree River at Columbia and Cayce downstream of the Saluda and Broad Rivers' confluence. The Lower Saluda River (S) samples were collected near Hope ferry landing (34°02′45.7″N 81°11′27.3″W), approximately 2.7 km downstream of Lake Murray reservoir dam and 12.9 km upstream of the Lower Saluda and Broad Rivers' confluence. The Broad River (B) water samples were collected near Columbia rowing club (34°02′36.9″N 81°04′23.7″W), which is approximately 4.5 km upstream of

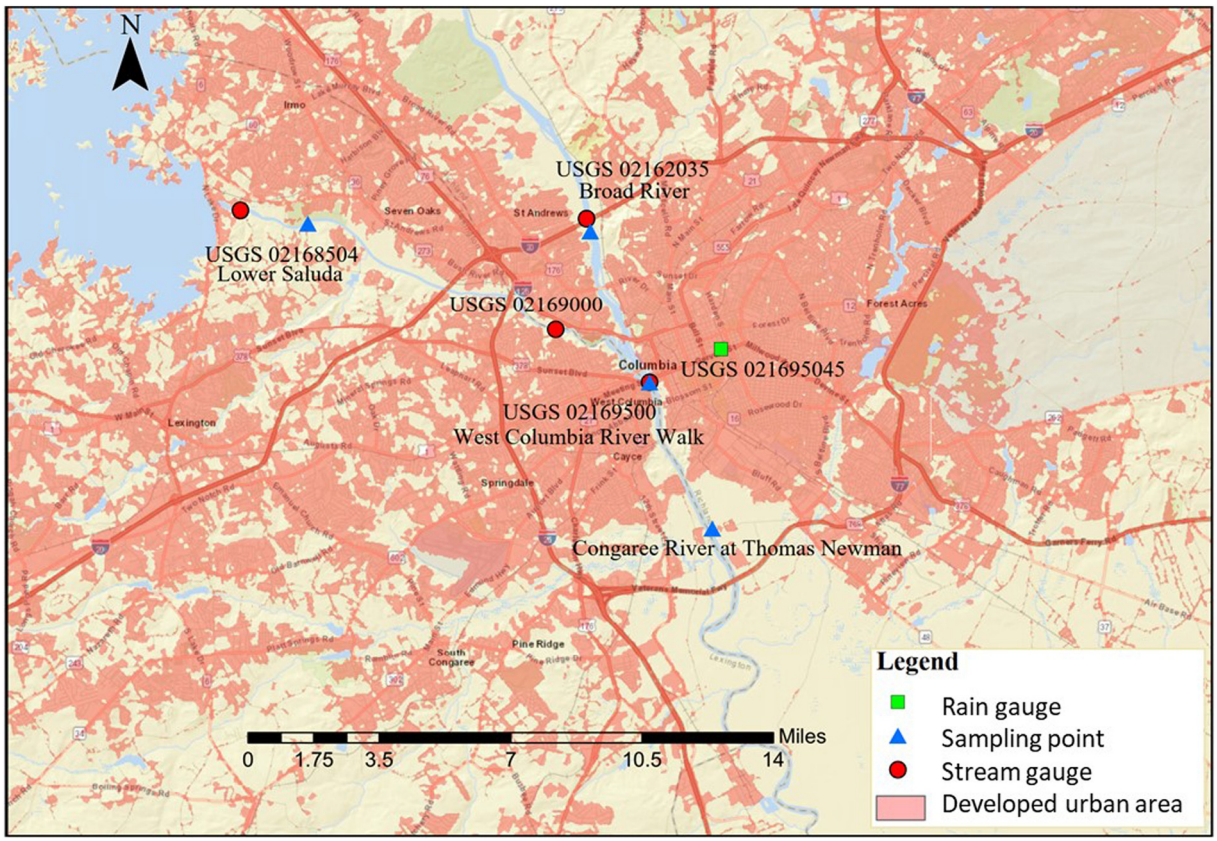

Fig. 1 Map of the city of Columbia, South Carolina displaying the developed urban area and the sampling locations at the Lower Saluda River (S), Broad River (B), Congaree River at Columbia (Co), and Congaree River at Cayce (C).

the Saluda and Broad Rivers' confluence. The Congaree River Columbia samples were collected at West Columbia Riverwalk (33°59′35.4″N 81°03′1.8″W, Co), which is approximately 1.5 km downstream of the Saluda and Broad confluence. The Congaree River Cayce samples were collected at Thomas Newman public boat landing (33°56′57.3″N 81°01′44.1″W, C), which is approximately 6.8 km downstream of the Saluda and Broad Rivers' confluence. This sampling area captures a significant footprint of the urban area – accounting for approximately 50% – of the city of Columbia, South Carolina, United States. A detailed description of the sampling locations including land use, industrial-commercial activities, mining activities, wastewater and storm water facilities in the watershed is provided in the ESI† Section S1.

Precipitation data for the Broad and Congaree Rivers' sampling locations was collected from the USGS station number 021695045 (34°00′24″N 81°01′18″W), nearly 6.3 km from the Broad River sampling location, and nearly 3.1 km from the Congaree River Columbia sampling location and 6.4 km from the Congaree River Cayce sampling location. Rainfall and discharge data for the Lower Saluda River sampling location were collected from USGS station number 02168504 (34°03′03″ N 81°12′35″W) immediately after the dam and nearly 1.8 km upstream from the Lower Saluda River sampling location. The discharge data for the Broad and Congaree Rivers was collected from the USGS stations' number 02162035 (34°02′54″N 81°04′ 24″W) and 02169500 (33°59′35″N 81°03′00″W), nearly 5.3 km upstream of the Broad River sampling location and 0.05 km upstream from the Congaree River Columbia sampling location and 5.3 km upstream from the Congaree River Cayce sampling location, respectively.

2.2. Sample collection, digestion, and elemental analysis

Surface water samples were collected from the Broad, Lower Saluda, and Congaree Rivers in 250 mL high density polyethylene bottles (Thermo Scientific, Rockwood, TN, United States). Prior to use, bottles were acid-washed in 10% nitric acid (Sigma Aldrich, St. Louis, MO, United States) for at least 24 hours, and soaked in ultrahigh purity water (PURELAB Option-Q, ELGA, High Wycombe, UK) for 24 hours, air dried, and double-bagged. In the field, sampling bottles were rinsed three times in the surface water and then filled with the water sample. Samples were individually double-bagged and returned to the lab the same day and stored in the dark at 4 °C.

The bulk water samples were digested using a mixture of H_2O_2, HNO_3, and HF following the digestion protocol described elsewhere and summarized in the ESI† Section S2.[17,22,37] Elemental concentrations in the digested samples were determined by icpTOF R ICP-TOF-MS (TOFWERK, Switzerland) using TOF Pilot 2.8.8 software. The instrument

operating conditions are presented in Table S3.† Mass spectra calibration and standard tuning procedure were performed before analysis for instrument maintenance. Dissolved multi-element standards were prepared in 1% HNO_3 from commercially available ICP standards (BDH Chemicals, Radnor, PA, USA) with concentrations ranging from 0.001 to 100 μg L^{-1}. Internal standards (ICP Internal Element Group Calibration Standard, BDH Chemicals, Radnor, PA, USA) were monitored at the same time for quality control. The isotopes measured were ^{27}Al, ^{49}Ti, ^{57}Fe, ^{90}Zr, ^{93}Nb, ^{139}La, ^{140}Ce, ^{141}Pr, ^{142}Nd, ^{152}Sm, ^{153}Eu, ^{158}Gd, ^{159}Tb, ^{164}Dy, ^{165}Ho, ^{166}Er, ^{169}Tm, ^{174}Yb, and ^{175}Lu. The minor isotopes (*e.g.*, ^{49}Ti and ^{57}Fe) instead of the major isotopes (*e.g.*, ^{48}Ti and ^{56}Fe) were used to determine the concentrations of Ti and Fe to avoid potential isobaric element and polyatomic ion interferences with $^{48}Ca^{+}$ and $^{40}Ar^{16}O^{+}$, respectively. All isotopes were analyzed in collision/reaction mode.

The USGS reference material BHVO-2 Hawaiian basalt was digested following the same procedure described above. The elemental analysis of the reference material demonstrated high recovery (approximately 100%) for most elements. The precision of our method was within 8% for all isotopes and the accuracy was better than 89% for most elements, including Ti and Nb. Full procedural digestion blanks was <6.8% samples' analyte signal for all reported element in this study and <2.8% samples' analyte signal for Ti and Nb (Table S4†). Therefore, blanks are insignificant to the calculations of Ti concentrations or total Ti/Nb elemental ratios.

2.3. Particle composition on single particle basis

The multi-elemental composition of individual particles in a select set of samples (*e.g.*, 30/4/2020, 1/5/2020, 2/5/2020, and 5/5/2020) representing the start, rising limp, peak, and end of the first runoff event in the studied river system was determined using SP-ICP-TOF-MS. The river water samples were shaken well prior to extraction to resuspend any settled particles and to obtain a representative subsample. The extraction procedure is the same as that used in previous studies.[17,22,37] Briefly, 10 mL aliquots of the river water samples were transferred into acid-washed 15 mL centrifuge tubes. Then, the samples were bath sonicated for 2 h (Branson, Model 2800, 40 kHz, Danbury, CT, United States) and centrifuged at 775*g* for 5 min (Eppendorf Centrifuge 5810R, Hamburg, Germany) to obtain the <1 μm particle size fraction (assuming natural particle density of 2.5 g cm^{-3}). The theoretical equivalent spherical diameter of the extracted fractions corresponds to particles <1000 nm for natural particles (ρ = 2.5 g cm^{-3}), and <725 nm for TiO_2 particles (ρ = 4.2 g cm^{-3}). All samples were bath sonicated again for 15 min and were diluted by a factor of 100 prior to SP-ICP-TOF-MS analysis.

Similar to the total elemental analysis, the instrument was calibrated and tuned daily before single particle analysis. Transport efficiency was calculated based on analysis of certified Au ENPs (NIST RM8013 Au, Gaithersburg, MD, USA) and ionic Au standards.[41] Dissolved element calibration was performed using a series of mixed multi-element standards (0, 1, 2, 5, and 10 μg L^{-1}, BDH Chemicals, Radnor, PA, USA). Particle signals were separated from baseline using TOF Pilot V2.10 and reported in time-elapsed format.

The detected particles were classified into single- and multi-metals (smNPs and mmNPs). The smNPs were considered as their own clusters because the particle mass and number concentrations are not sufficient to cluster smNPs. The mmNPs were classified into clusters of NPs of similar elemental composition using a two stage – intra- and inter-sample – agglomerative hierarchical clustering algorithm in MATLAB following the method described elsewhere.[42] Briefly, intra-sample hierarchical clustering was performed – using average correlation distance – on all metal masses in each NP to generate clusters that best account for variance in NP metallic composition in each sample. This step generates a cluster dendrogram for each sample, which was divided into major clusters using a distance cutoff. The distance cutoff of 0.65, was determined by visually inspecting the dendrogram and through trial and error in order to minimize the variance/diversity in NP elemental composition in the major clusters. A cluster representative was determined for each major cluster as the mean of metal mass in individual NPs within each cluster taking into account all elements that occurred in at least 5 percent of NPs within the cluster. For each major cluster, the mass fraction of a given metal in each particle was determined as the mass of that metal divided by the sum of masses of all metals in that NP. The inter-sample clustering was performed on the major cluster representatives identified in the intra-sample clustering to group/cluster the similar NP major clusters identified in the different samples. This step generates a cluster dendrogram for intra-sample cluster representatives, which was divided into major clusters using a distance cutoff as performed for the intra sample clusters. The distance cutoff of 0.2, was determined by visually inspecting the dendrogram and through trial and error in order to minimize the variance/diversity in the cluster representative elemental composition in the major clusters. The mean intra-sample cluster composition was determined as the mean of metal mass fraction in all NPs in the cluster and was compared across samples. Select elemental ratios were determined on a particle-per-particle basis taking into account all particles containing the two elements. The number concentration (NP g^{-1}) of the total, smNPs, mmNPs, and cluster members were determined according to the SP-ICP-MS theory.[41]

2.4. Estimation of TiO_2 engineered particle concentration

The concentration of TiO_2 engineered particles was calculated based on mass balance calculations according to eqn (1)

$$[TiO_2]_{\text{engineered particles}} = \frac{TiO_{2\ MM}}{Ti_{MM}}\left[Ti_{\text{sample}} - Nb_{\text{sample}} \cdot \left(\frac{Ti}{Nb}\right)_{\text{background}}\right] \quad (1)$$

where, $[TiO_2]_{\text{engineered particles}}$ is the concentration of TiO_2 engineered particles (μg L^{-1}), Ti_{MM} and $TiO_{2\ MM}$ are the molar

masses of Ti and TiO_2, Ti_{sample} and Nb_{sample} are the concentrations ($\mu g\ L^{-1}$) of Ti and Nb in a given sample, $(Ti/Nb)_{background}$ is the natural background elemental concentration ratio of Ti/Nb. Background Ti/Nb was calculated on eight reference samples collected from Lake Katherine and Gills creek in Columbia, SC in the absence of rainfall events.[20] Eqn (1) assumes that all Ti occurs in particulate form, engineered Ti occurs as pure TiO_2 engineered particles, and that the natural background Ti/Nb is constant throughout the sampling period. These assumptions are justified for the following reasons. Ti occurrence in the surface waters is expected to occur solely in solid phases because of the very low solubility of TiO_2.[43] While Ti has numerous industrial applications, from metal alloying to aerospace applications to biomedical devices, approximately 95% of the mined Ti is refined into nearly pure TiO_2 through the treatment of Ti-bearing ores with carbon, chlorine, or sulfuric acid.[44] Additionally, TiO_2 engineered particle contain trace amount of Nb, which was below the ICP-MS detection limit (*e.g.*, $<7\ ng\ L^{-1}$) for TiO_2 concentration upto 10 000 $mg\ L^{-1}$.[22] On the other hand, natural TiO_2 minerals are the dominant carriers (*e.g.*, >90–95% of the whole rock content) of Ti and Nb. The elemental ratios of Ti/Fe, Ti/Al, Ti/Ce, Ti/Zr, and Ti/Nb, determined by SP-ICP-TOF-MS, in naturally occurring particles in the Broad, Lower Saluda, and Congaree Rivers were found to be within the range of naturally occurring particles throughout the sampling campaigns (see discussion below and ESI†).

2.5. Discharge hydrographs and baseflow estimation

The discharge was separated into baseflow and direct runoff using the tool "WHAT: Web-based Hydrograph Analysis Tool". 'WHAT' is able to connect to the USGS database and query and analyze streamflow data based on its USGS gauge number. The baseflow and direct runoff separation for the Broad, Lower Saluda, and Congaree Rivers was performed for the USGS station number 02162035, 02168504, and 02169500, respectively. For baseflow separation, recursive digital filter has been used with aquifer type of perennial streams with porous aquifer.

3. Results

3.1. Precipitation, discharge, runoff, and water quality

A significant rain event occurred on 30/4/2020 resulting in 16.8 mm, 15.7 mm, and 16.8 mm rainfall in the Broad, Lower Saluda, and Congaree River watersheds respectively. Smaller rain events of 0.5, 0.5, and 1.0 mm occurred on 29/4/2020, 5/5/2020, and 10/5/2020 in the Broad, Lower Saluda, and Congaree River watersheds, respectively (Table S5†). Moreover, major rainfall events of 40.2 mm and 9.7 mm occurred on 29/4/2020 in the upstream region of the Broad River at Ashville, NC and Knoxville, TN respectively;[45,46] and 54.5 mm and 3.1 mm occurred on 29/4/2020 and 30/4/2020 in the upstream region of the Lower Saluda River at Rock reservoir, Cleveland, SC.[47] These rain events resulted in increases in release from upstream reservoirs and as a result increases in the discharge in the Lower Saluda, Broad, and Congaree Rivers (Table S5; Fig. S1†). During this period, water level behind the Lake Murray dam was about 109 m above datum, which is very close to the top of conservation (flood control level of ~109.1 m) of the dam. The discharge in the Lower Saluda River is dominated by regulated releases from the Lake Murray reservoir based on the required hydroelectric power generation and flood control regulations. Thus, the discharge in the Lower Saluda River displayed sharp increases between 30/4/2020 and 1/5/2020 and between 4/5/202 and 9/5/2020 due to releases from the Lake Murray reservoir in anticipation of the rain events to keep water level behind the dam below flood zone level (Table S5; Fig. S1†). Lake Murray is a man-made reservoir of approximately 200 km^2 in size with a maximum depth of approximately 53 m, an average depth of approximately 14 m, and a residence time of approximately 417 days.[48,49] The majority of the inflow to Lake Murray comes from releases from upstream dams on Saluda River as well as rainfall over the lake. Local tributaries, which are mostly rural basins, contribute minimally to the storage behind the Lake Murray dam. Thus, the urban contribution at the sampling point to the total discharge is minimal.

The discharge in the Broad and the Congaree Rivers display typical hydrographs of natural river discharges. The Broad River is regulated to some degree by the presence of at least 10 hydroelectric facilities and two thermoelectric power plants (Table S1†).[50] The upstream of Broad River from sampling point is regulated by low the Parr reservoir dam, approximately 40 km upstream of the sampling location, which operates in modified run-of-river mode and operates continuously to pass the Broad River flow. These facilities allow a natural river flow to downstream.[51] The retention time of Parr Reservoir is on average about 3 days and varies between 0.8 and 29.3 days based on a maximum and minimum monthly flow of 530 and 15 $m^3\ s^{-1}$, respectively.[52] The nearest dam to the sampling location is the Broad River diversion dam (low head, a constructed barrier in a river with a hydraulic height not exceeding 7.6 m), approximately 4 km upstream of the Broad River sampling site. This dam diverts the flow (long term average diversion of approximately 11.7 $m^3\ s^{-1}$) of the Broad River toward the canal of the Columbia Hydroelectric Project. The rainfall resulted in runoff discharges in the Broad and Congaree Rivers between 30/4/2020 and 4/5/2020 and between 5/5/2020 and 9/5/2020 with peak discharge on 1/5/2020 and 7/5/2020. Direct runoff accounted for <6%, 9–77%, 8–75% of the total discharge in the Lower Saluda, Broad, and Congaree River, respectively. The highest runoff contribution (*e.g.*, direct runoff/total discharge) in the Broad and Congaree Rivers occurred on 1/5/2020. There has been no urban runoff contribution (*i.e.*, baseline flow occurred) on 27/4/2020, 10/5/2020, and 12/5/2020 in the Broad and Congaree Rivers. The average annual discharge rates at the Broad River and Congaree River Columbia sampling sites are approximately 163.08 $m^3\ s^{-1}$ and 243.86 $m^3\ s^{-1}$. We estimated the urban contribution from the city of

Columbia between the Broad and Congaree Rivers' sampling sites as the difference between the sum of the discharge at the Congaree River sampling location and the water withdrawal at the Broad River diversion dam (approximately 255.56 m^3 s^{-1}) and the sum of the discharge at the Broad River and Lower Saluda River sampling locations (approximately 225.68 m^3 s^{-1}). The average annual runoff contribution of the city of Columbia is approximately 29.88 m^3 s^{-1}.

The pH varied in a narrow range between 6.4 and 7.8 and is similar in all samples (Fig. S2a†). The conductivity vary between 48 and 119 μs cm^{-1} with higher values on 27/4/2020 and 28/4/2020 and relatively stable values of around 55 μs cm^{-1} between 29/4/2020 and 12/5/2020 (Fig. S2b†). The water temperature in the Lower Saluda River water was lower than those in the Broad and Congaree Rivers as the water comes from deep in Lake Murray reservoir (Fig. S2c†).

3.2. Total Ti, Nb, and TiO_2 concentrations

Titanium and Niobium concentrations in the Lower Saluda, Broad, and Congaree Rivers during the sampling period are presented in Fig. 2a and b. Titanium concentrations vary randomly within a narrow range in the Lower Saluda River between 13 and 60 μg L^{-1} (Fig. 2a) and does not follow a specific trend in relation to the discharge. In contrast, titanium concentrations vary within a broader range in the Broad and Congaree Rivers at Columbia and Cayce (8 to 926 μg L^{-1}, 95 to 5976 μg L^{-1}, and 58 to 1170 μg L^{-1}, respectively). The concentrations of Ti in the Broad River follow the discharge trend and continue rising after the second discharge peak. The reason for the increase in Ti concentration after the second discharge peak is unknown. The concentrations of Ti in the Congaree River at Columbia and Cayce display a bimodal distribution and follow closely the rise and fall of the discharge. The highest Ti concentration in the Congaree River at Columbia and Cayce was measured on 1/5/2020 and 2/5/2020, respectively. Generally, Ti concentrations decrease following the order: Congaree River at Columbia > Congaree River at Cayce > Broad River > Lower Saluda River, which is scribed to differences in Ti load into these rivers due to differences in urban runoff contribution to the total discharge. The Nb concentrations follow the same trend as that of Ti (Fig. 2b). Ti and Nb pollutographs in the Broad and Congaree Rivers display a mobility pattern driven by the transport of solids;[53] that is the Ti and Nb concentrations are low during low flows, increase with increasing flow due to the transportation of more solids, and then decline with diminishing flow and supply of solids on the catchment surfaces (Fig. 2).

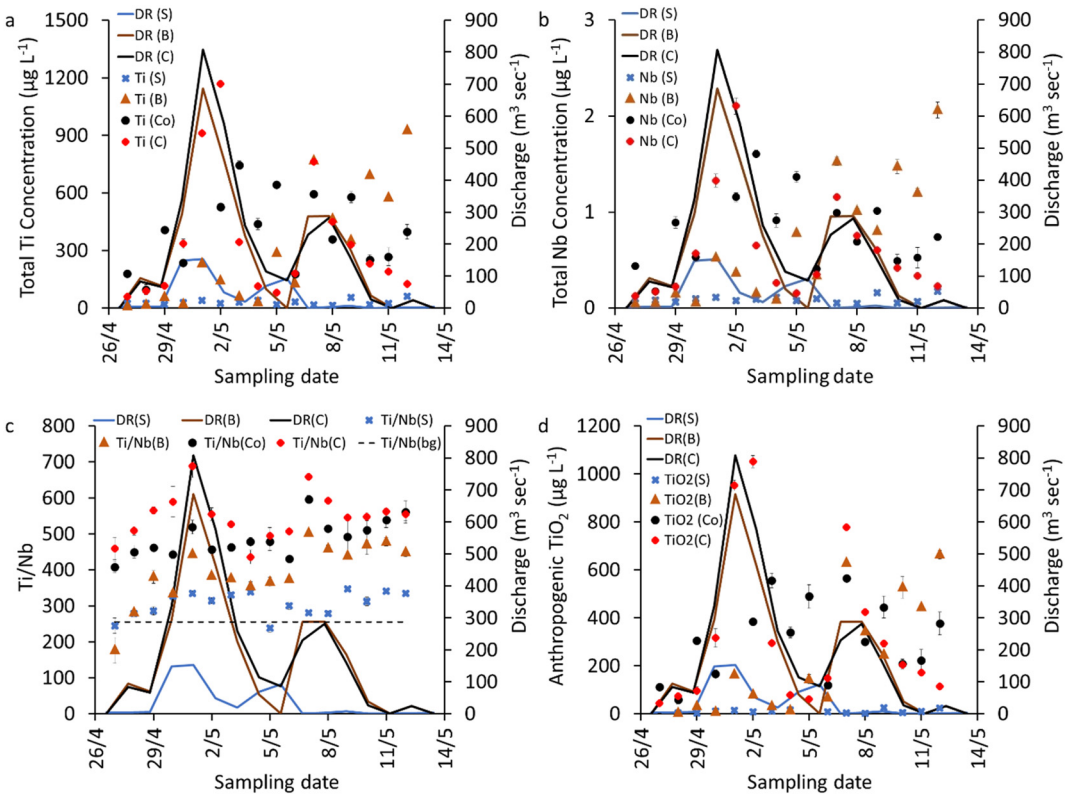

Fig. 2 Pollutographs of (a and b) the total concentrations of Ti and Nb, (c) Ti/Nb, and (d) the estimated anthropogenic TiO_2 concentrations in the Lower Saluda River (S), the Broad River (B), and the Congaree River at Columbia (Co) and Cayce (C) during the sampling campaign. DR (S) refers to direct runoff in the Lower Saluda River, DR (B) refers to direct runoff in the Broad River, and DR (Co) refers to direct runoff in the Congaree River at Columbia. The highest Ti, Nb, and TiO_2 concentrations in the Congaree River at Columbia was 5976 ± 89, 11.5 ± 0.5, 5050 ± 143 μg L^{-1} on 1/5/2020 and are not displayed in the figure.

In the Lower Saluda River, the Ti/Nb ratios vary between 238.8 ± 12.1 and 346.7 ± 2.4 and do not follow specific trend with the discharge (Fig. 2c). In the Broad and Congaree Rivers, the Ti/Nb ratios display a bimodal distribution and increase with increases and decreases in the discharge/runoff. The general increase in Ti/Nb ratios over time can be attributed to the continuous runoff input during the sampling period. The Ti/Nb values increase following the order Lower Saluda River < Broad River < Congaree River at Columbia < Congaree River at Cayce. This trend in Ti/Nb ratios is attributed to the introduction of anthropogenic pure Ti-bearing particles between the sampling sites, which can be ascribed to urban runoff from the city of Columbia. The concentration of the anthropogenic Ti-bearing particles was estimated using mass balance and assuming that they occurred as pure TiO_2 particles. The estimated anthropogenic TiO_2 concentrations vary between 0 and 24 μg L^{-1} in the Lower Saluda River, 0 and 663 μg L^{-1} in the Broad River, 58 and 5050 μg L^{-1} in the Congaree River at Columbia, and 43 to 1051 μg L^{-1} in the Congaree River at Cayce; and follow the same trend with discharge/direct runoff as the total Ti concentrations (Fig. 2d).

3.3. Particle number concentrations and elemental composition

The number concentrations of Ti-bearing particles are generally higher in the Broad and Congaree Rivers compared to those in the Lower Saluda River (Fig. 3a). The relative abundance of smTi-NPs is generally higher during the first discharge event than at the end of the event (Fig. 3b). All other elements follow the same trend as Ti-bearing particles (Fig. S3†). Due to the complex nature of the SP-ICP-TOF-MS, only a select set of four samples per sampling site during the first discharge peak were analyzed to determine the elemental composition of NP at the single particle level. Therefore, it is not possible to compare the relative abundance of smNPs before the discharge to that during the discharge peak. The mass distributions of Ti-bearing particles vary within the same range (*e.g.*, 0 to 20 fg) in all samples (Fig. 4). However, the mass distributions of Ti-bearing particles in the Broad and Congaree Rivers display a shift toward larger masses compared to those in the Lower Saluda River, with a higher fraction of particles with mass >20 fg. The mass distributions of Ti-bearing particles in the Congaree River at Columbia is intermediate between those in the Broad and the Lower Saluda Rivers due to the mixing of the two Rivers upstream of this sampling location (Fig. 4). The mass distributions of Ti-bearing particles shift toward higher masses during high discharge (1/5/2020 and 2/5/2020) compared to those at low discharge (30/4/2020 and 5/5/2020). The mass distributions of smTi and mmTi-bearing particles cover the same mass distribution range with a higher abundance of Ti particles with larger masses for mmTi-bearing than smTi-bearing particles (Fig. S4†). This can be attributed to the higher probability of detecting naturally occurring elements in natural mmTi-bearing particles or to the heteroaggregation of smTi- and mmTi- or the heteroaggregation of multiple mmTi-bearing particles.

Clustering analysis of the mmNPs identified 29 mmNP clusters. Six of these 29 clusters – FeTiMn, AlSiFe, CeLaNd, TiMnFe, MnCeBa, and ZrYTh – occur in all samples and account for >99.4% of the total number of mmNPs in all samples (Fig. S5†). The elemental composition of these clusters is dominated by one element and contain minor or trace concentrations of other elements (Fig. 5).[54] The Ti-bearing particles are distributed among three clusters: FeTiMn, AlSiFe, and TiMnFe, which account for >99% of all mm-Ti-bearing NPs (Fig. S5†). The elemental ratios of Ti/Fe, Ti/Al, Ti/Ce, Ti/Zr, and Ti/Nb are similar in all samples and are in good agreement with those measured in natural soils and surface waters (Fig. S6–S8†).[20,54,55] The median values of Ti/Fe, Ti/Al, Ti/Ce, Ti/Zr, and Ti/Nb varies within the range of those measured in of natural soils and surface waters (Tables

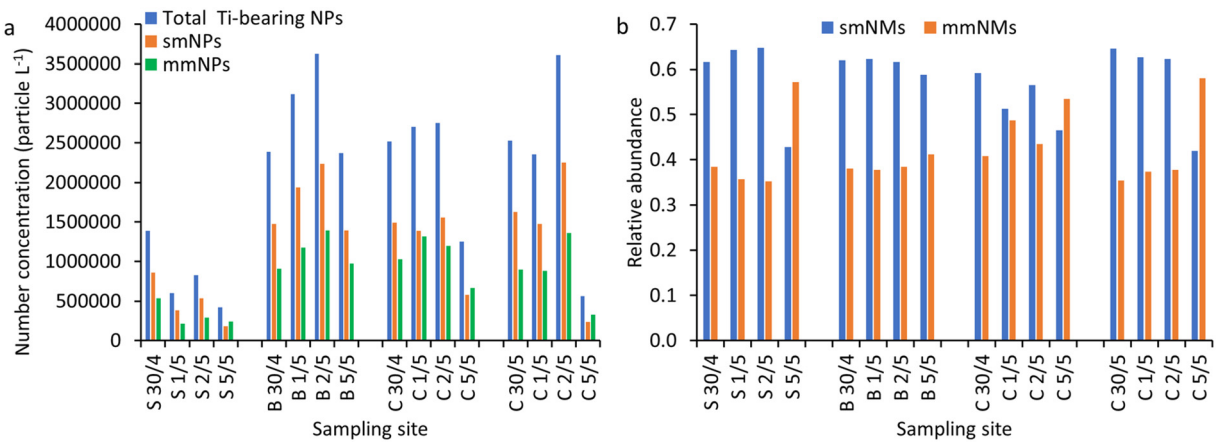

Fig. 3 (a) Number concentration of total, single metal (sm) and multi-metal (mm), and (b) the relative abundance of sm- and mm-Ti-bearing nanoparticles in the Lower Saluda River (S), Broad River (B), Congaree River at Columbia (Co), and Congaree River at Cayce (C). The number concentrations were corrected by subtracting the number of particles detected in the procedural blanks.

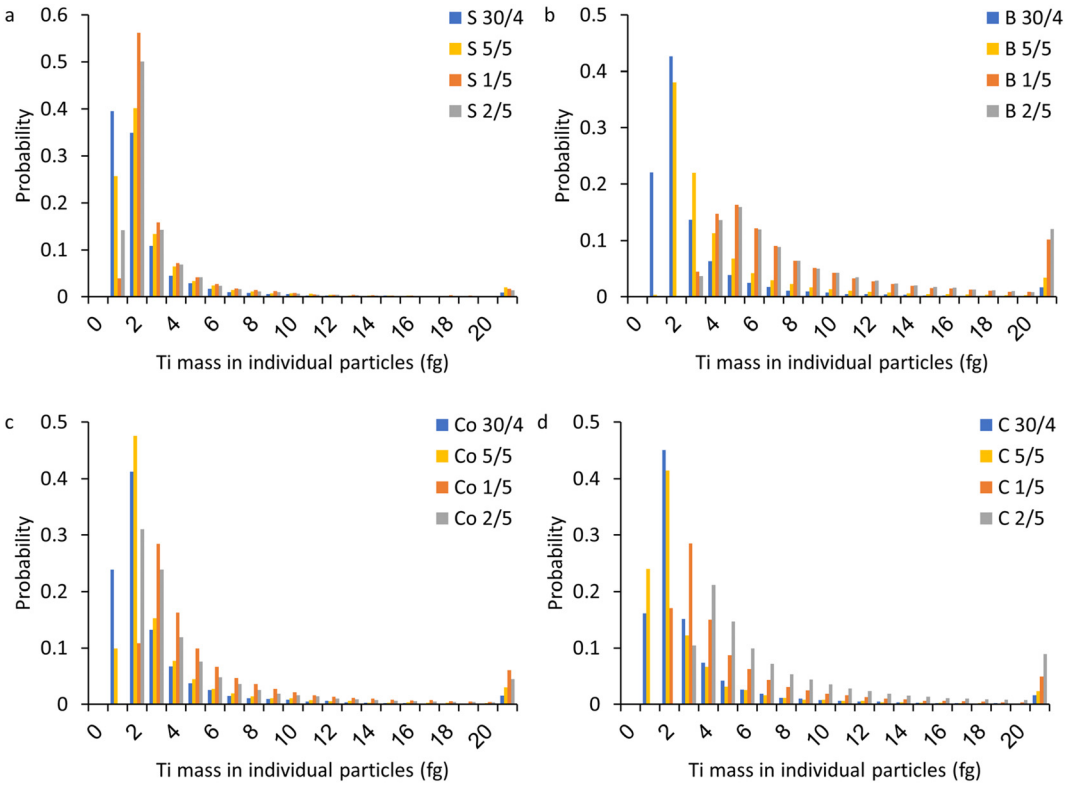

Fig. 4 Mass distribution of Ti-containing particles in the: (a) Lower Saluda River, (b) Broad River, (c) Congaree River at Columbia, (d) Congaree River at Cayce. S: Lower Saluda River, B: Broad River, Co: Congaree River at Columbia, and C: Congaree River at Cayce.

S6–S8†).[20,54,55] The mean Ti/Nb ratio in all Ti and Nb containing particles in all samples vary between (mean ± standard deviation of the ratios calculated at the single particle level) 218 ± 195 and 295 ± 280.

4. Discussion

The lowest Ti concentration in the Lower Saluda, Broad, and Congaree (Co) Rivers are 13.3 ± 0.2 μg L^{-1}, 8.2 ± 0.1 μg L^{-1}, and 94.8 ± 27.1 μg L^{-1} respectively and occurred during base flow dominated condition when base flow accounted for 90.5%, 100%, and 68% of the total discharge, respectively (Fig. 2a). The highest Ti concentration in the Lower Saluda, Broad, and Congaree (Co) Rivers are 39.2 ± 6.7 μg L^{-1}, 233.4 ± 8.1 μg L^{-1} and 5975.7 ± 88.8 μg L^{-1} respectively and coincided with the peak discharge during the first runoff event on 1/5/2020 (Fig. 2a). The low concentration of Ti in the Saluda River, which is characterized by minimal urban runoff contribution to the total discharge, and the increase in Ti concentration from the Broad River to the Congaree River, which are characterized by high urban runoff contribution to the total discharge, suggest that urban runoff is the key driver of Ti concentrations in the Broad and Congaree Rivers. The Ti concentrations measured in this study are higher than those previously measured in rivers (*e.g.*, 0.6 to 1.6 μg L^{-1}),[56] urban runoff (*e.g.*, 10 to 15 μg L^{-1}) following the release of TiO_2 particles from exterior facades,[57] and urban wet and dry runoff (*e.g.*, 15 to 200 μg L^{-1}).[17] Nonetheless, higher Ti concentrations (*e.g.*, 12.7 mg L^{-1}) were reported in highway runoff in Pullman, Washington.[19] Additionally, high Ti concentrations (*e.g.*, 150 to1600 mg kg^{-1}) were reported in different road-environment samples (*e.g.*, road dust, sludge from storm drains, and roadside soil), which were suspected to be of anthropogenic origin such as the use of alkali metal titanates as inorganic fillers for the purpose of stabilizing the friction coefficient.[58]

Titanium in urban runoff can be attributed to natural and/or anthropogenic sources. Significant quantities of Ti-bearing particles occur in the urban environment due to the soil erosion and atmospheric deposition of soil particles on surfaces in the urban environment.[59] On the other hand, TiO_2 engineered particles are widely used in many applications in the urban environment as pigment in paint and coatings[60,61] and as ENPs in self-cleaning surfaces which have been shown to be released by wear and weathering.[5–9] Several studies reported the occurrence of TiO_2 engineered (nano)-particles in road dust, atmospheric particulate matter,[62,63] and urban runoff.[17] Whereas naturally occurring TiO_2 minerals are the dominant carriers of Ti and Nb,[34] commercial TiO_2 particles are typically refined into nearly pure TiO_2.[22,64] Thus, the elemental ratio of Ti/Nb was used to determine whether the increased Ti concentration is due to natural or anthropogenic Ti inputs. The Ti/Nb in most samples is higher than the natural background ratio determined in a previous study (Fig. 2c),[20] suggesting that all sampling locations received anthropogenic Ti inputs. The

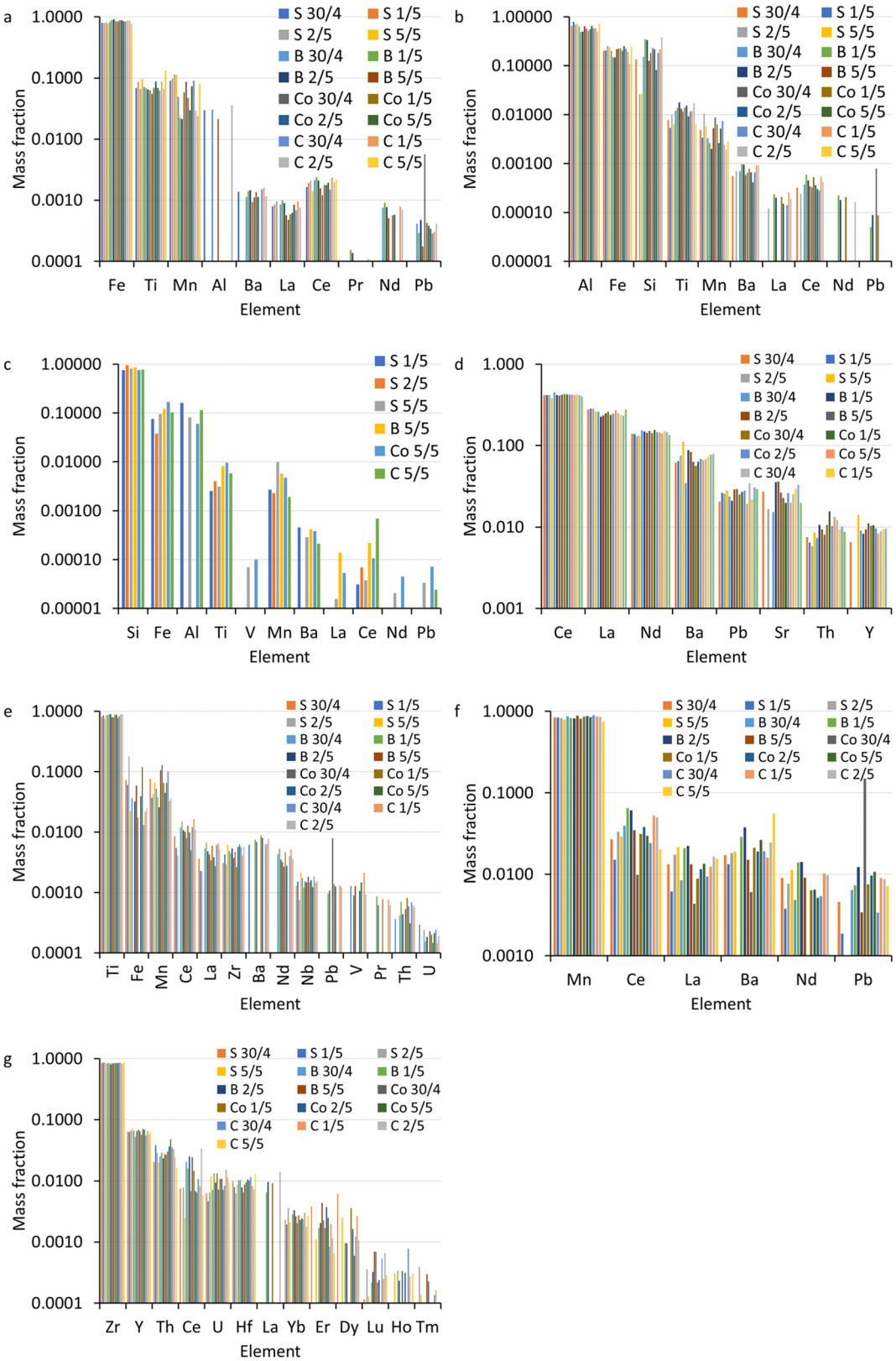

Fig. 5 Elemental composition of the dominant clusters: (a) Fe-, (b) Al-, (c) Si-, (d) Ce-, (e) Ti-, (f) Mn-, and (g) Zr-rich particle cluster. Standard error was <0.05 for all elements. Note that the Al and Si-rich mmNP clusters are two clusters within the AlSiFe cluster. S: Lower Saluda River, B: Broad River, Co: Congaree River at Columbia, and C: Congaree River at Cayce.

lowest Ti/Nb ratios occurred in the Lower Saluda River (239 ± 12) and coincided with the average water background Ti/Nb determined in nearby water bodies (266 ± 9).[20] The higher (*e.g.*, 280–346) Ti/Nb values in the Lower Saluda River indicate a potential small anthropogenic contribution of TiO_2 engineered particles, potentially from atmospheric deposition or urban runoff from nearby roads and bridges. The lowest Ti/Nb in the Broad and Congaree Rivers (177 ± 36, 408 ± 17, and 435 ± 19, respectively) occurred at the base flow conditions. On the other hand, the highest Ti/Nb ratios (503 ± 5, 596 ± 11, and 688 ± 31) occurred at the peak of the discharge events on 1/5/2020 and 7/52020, suggesting that the discharge/urban runoff is the driver of the increase in Ti/Nb during/following rainfall events. The lower Ti/Nb ratios in the Lower Saluda River than in the Broad and Congaree Rivers are ascribed to the smaller urban runoff contribution to the Lower Saluda River discharge at the sampling location along with sedimentation of anthropogenic Ti-bearing particles in Lake Murray, and thus low input of anthropogenic Ti to the Lower Saluda River.

The anthropogenic Ti-bearing particles from urban runoff can occur as smNPs such as those used in building paint, road marking, and photocatalytic surfaces or as mmNPs as those released from traffic-related emissions such as Ti used as fillers in brake pads. Thus, SP-ICP-TOF-MS analysis was used to determine the elemental composition of Ti-bearing particles. The SP-ICP-TOF-MS analysis show higher relative abundance of smTi-bearing NPs during the runoff event than at the end of the runoff event (Fig. 3b) in all sampling sites, which can be ascribed to the increased contribution of pure TiO_2 particles to the total concentration of Ti-bearing particles during the runoff event. The clustering and elemental ratio analysis show that >99% of mm-Ti-bearing particles occurred in three clusters (FeTiMn, AlSiFe, TiMnFe), which are typical of naturally occurring particles such as titanomagnetite (Ti/Fe = 0 to 0.43), ilmenite (Ti/Fe = 0.86), pseudorutile (Ti/Fe = 1.29), ilmenorutile (Ti/Fe = 1.71), or altered pseudorutile (Ti/Fe > 1.71) (Fig. S6a and S7a†), clays (Ti/Al = 0 to 0.4, Fig. S6a and S7a†), or titanium oxide particles containing Al and Fe (Fig. S8†). The higher bulk Ti/Nb than the natural background ratio and the absence of any signature of anthropogenic mmTi-bearing NPs suggest that the majority of anthropogenic Ti-bearing particles are pure TiO_2 particles. It is worth noting that other clusters such as Zn, Cu, Cr, W, Ni, Sn-rich particle clusters were identified more frequently in the Broad and Congaree Rivers than in the Lower Saluda River (Fig. S5†). These particles are typical of traffic related emissions detected in bridge runoff in Columbia, South Carolina.[36] However, the number of the detected particles are relatively small and thus these clusters are not discussed further.

Consequently, the total TiO_2 engineered particle concentrations were determined using mass balance calculations and shifts in Ti/Nb above the natural background values (Fig. 2d). The lower concentrations of TiO_2 engineered particles in the Lower Saluda River compared to the Broad and Congaree Rivers can be attributed to the removal of suspended sediments and anthropogenic TiO_2 particles within the Lake Murray reservoir by sedimentation given the long water residence time of approximately 417 days.[48,49] This is consistent with the decreases in turbidity from upstream to downstream Lake Murray reservoir.[48,49] This is also consistent with the smaller masses of Ti-bearing particles in the Lower Saluda River compared to those in the Broad and Congaree Rivers (Fig. 4). Additionally, the low TiO_2 concentrations in the Lower Saluda River can be attributed to the absence or small urban runoff contribution (~6%) to the discharge at the Lower Saluda River sampling location. In contrast, the Broad River is a natural free flowing river which transports a high sediment loads into the Broad River sampling location from the large upstream Broad River watershed. Additionally, the Broad River sampling site is approximately 480 m downstream of a major highway in South Carolina – that is the interstate I20 bridge – which discharges directly into the Broad River. Our previous study demonstrated that bridge runoff contains high concentrations of anthropogenic TiO_2 particles.[65]

The increase in TiO_2 concentration from the Broad River to the Congaree River for most sampling dates suggests that the majority of anthropogenic TiO_2 is introduced into the Broad and Congaree Rivers at the urban interface area of the city Columbia, SC, and is ascribed to urban runoff and associated particulate wash off from impervious surfaces. This is consistent with the significant contribution of urban runoff to the total discharge in the Broad (*e.g.*, 9–77%) and the Congaree (*e.g.*, 8–75%) Rivers as well as the high concentrations of TiO_2 in bridge and urban runoff.[17] The Broad River samples were collected downstream of the I20 highway; the Congaree River at Columbia samples were collected downstream of I176, I126, the Jarvis Klapman Boulevard, and the Gervais Bridges; and the Congaree River at Cayce samples were collected downstream of Blossom Street Bridge. All these bridges have an AADT >20 000, which result in a substantial release of TiO_2 to the studied river system (Table S2†). For instance, the Blossom Street Bridge (AADT = 27 500) runoff has been shown to contain up to 101.1 ± 1.4 μg TiO_2 per L.[36] It is expected that bridges with higher traffic density will release higher concentrations of TiO_2 to the studied river system. The lower TiO_2 concentration in the Congaree River than in the Broad River between 10/5/2020 and 12/5/2020 could be due to dilution effect because of the mixing of the Broad River water containing high TiO_2 concentrations with the Saluda River water containing low TiO_2 concentrations.

The higher TiO_2 concentrations during the first discharge peak than during the second discharge peak in the Congaree River are attributed to the relatively longer antecedent dry period (Table S5†) prior to the first rainfall event. Longer antecedent dry periods lead to higher contaminant accumulation on impervious surfaces in the watershed. The heavy rain event on the 29/4/2020 and 30/4/2020 throughout the watershed might have transported the accumulated

contaminants from the impervious surfaces into the river system. Similar increases in the Ti concentrations[22] and particulate matter associated contaminant (*e.g.*, metals) concentrations[66,67] with increases in antecedent dry period were observed for road runoff and urban runoff, respectively.

Although we attribute TiO_2 to urban runoff, other sources of TiO_2 engineered particles into surface waters include recreational activities in the watershed,[68] industrial discharge,[23] or construction activities,[69] effluents from wastewater treatment plant (WWTP),[70] and sanitary sewer overflows.[20] The recreational source (*e.g.*, use of sunscreen during bathing) can be ruled out because there was not any recreational activities in the three rivers during the sampling period due to 'coronavirus stay-at-home order' in South Carolina.[71,72] The industrial and construction sources also can be ruled out as there was no known industrial discharge sources and construction activities near the sampling locations which would result in a continuous discharge of TiO_2 particles to surface water. The human waste source is an insignificant source of TiO_2 to the river system during the sampling period because of the small size (1.1 ± 0.0 to 2.1 ± 0.1) of the gadolinium anomaly (Fig. S9†). Gadolinium anomaly is widely used to track effluent from wastewater treatment plants.[73] Previous studies reported gadolinium anomaly sizes between 1.0 and 30.0 (Table S9†) in river streams, and an anomaly >1.5 has been used as an indicator of wastewater treatment effluent in rivers. Consequently, the observed TiO_2 engineered particles contamination in this study is attributed to rainfall events followed by runoff introduction in the rivers, suggesting that the source of TiO_2 particles here is diffuse urban runoff across the Broad and Congaree Rivers' watersheds.

5. Conclusion

The daily monitoring of the total elemental concentrations, bulk elemental ratios, the number particle concentration, and the multi-element composition of single particles in the Saluda–Broad–Congaree Rivers' ecosystem highlights the presence, transient nature, and transport of anthropogenic TiO_2 engineered particle in this urban river ecosystem. The concentrations of TiO_2 engineered particle are lowest (0 to 24 μg L^{-1}) in the Lower Saluda River which has the lowest urban footprint. The TiO_2 engineered particle concentrations increase from the Broad River (0 to 663 μg L^{-1}) to the Congaree River (53 to 5050 μg L^{-1}) indicating a continuous and increased introduction of TiO_2 engineered into the Broad and Congaree Rivers with urban runoff from the urban area of the city of Columbia, South Carolina. Increases in TiO_2 concentrations are transient and coincided with rainfall with highest concentrations at or near the peak of the discharge. Thus, the urban environment represents a major source of TiO_2 engineered particle into surface waters. The high TiO_2 concentrations in the Broad–Congaree Rivers may pose environmental risk in this river ecosystem, and in other urban rivers, during and following rainfall events, in particular at and near peak discharge. Higher concentrations of TiO_2 engineered particles, and thus higher environmental risks, can be expected in more highly urbanized watersheds than the studied urban river ecosystem. The impact of these TiO_2 engineered particles on river organisms should be further evaluated, including investigating the effect (bioavailability and toxicity) of TiO_2 engineered particles on several organisms in the trophic chain using environmentally relevant concentrations, environmentally relevant particle aggregates, and considering frequent pulse *vs.* chronic exposure. The design of this study highlights the importance of selecting sampling sites and monitoring the spatiotemporal variations in engineered particle concentrations in surface waters for a more comprehensive understanding of the environmental fate, behavior, and risk assessment of engineered particles. To provide even a more detailed understanding of TiO_2 engineered particle fate and transport in urban ecosystems, future studies could include additional sampling sites, collect samples at higher time resolution or over longer sampling periods, collect data following storm events with various intensities and antecedent dry periods, and collect and analyze sediments samples to determine particle sedimentation and deposition in the river system.

Author contributions

Dr. Nabi and Dr. Wang performed the field work and collected the water samples. Dr. Nabi performed sample digestion and total metal concentration analysis and wrote the first draft. Dr. Wang performed single particle analysis. Mr. Erfani and Dr. Goharian developed the clustering analysis code. Dr. Mohammed Baalousha conceived the overall idea of the research, secured the funding, coordinated the collaboration among the research team, supervised Dr. Nabi and Dr. Wang in performing experimental work and data analysis. All authors contributed to the writing and editing of the manuscript.

Conflicts of interest

The authors declare that they have no known competing financial interests or personal relationships that could have appeared to influence the work reported in this paper.

Acknowledgements

This work was supported by the US National Science Foundation CAREER (1553909) grant to Dr. Mohammed Baalousha.

References

1 A. Müller, H. Österlund, J. Marsalek and M. Viklander, The pollution conveyed by urban runoff: A review of sources, *Sci. Total Environ.*, 2020, **709**, 136125.

2 F. von der Kammer, *et al.*, Analysis of engineered nanomaterials in complex matrices (environment and biota): General considerations and conceptual case studies, *Environ. Toxicol. Chem.*, 2012, **31**, 32–49.

3 M. Baalousha, *et al.*, Outdoor urban nanomaterials: The emergence of a new, integrated, and critical field of study, *Sci. Total Environ.*, 2016, **557–558**, 740–753.

4 Coatingsworld, Demand for Paint and coatings to reach 1.4 Billion Gallons in 2019|Statista, 2019, Available at: **https://www.statista.com/statistics/684695/united-states-paint-and-coatings-demand-by-market/**, (Accessed: 22nd April 2020).

5 D. Göhler, M. Stintz, L. Hillemann and M. Vorbau, Characterization of Nanoparticle Release from Surface Coatings by the Simulation of a Sanding Process, *Ann. Occup. Hyg.*, 2010, **54**, 615–624.

6 I. K. Koponen, K. A. Jensen and T. Schneider, Comparison of dust released from sanding conventional and nanoparticle-doped wall and wood coatings, *J. Exposure Sci. Environ. Epidemiol.*, 2011, **21**, 408–418.

7 A. W. Nored, M. C. G. Chalbot and I. G. Kavouras, Characterization of paint dust aerosol generated from mechanical abrasion of TiO2-containing paints, *J. Occup. Environ. Hyg.*, 2018, **15**, 629–640.

8 N. Shandilya, O. Le Bihan, C. Bressot and M. Morgeneyer, Evaluation of the Particle Aerosolization from n-TiO_2 Photocatalytic Nanocoatings under Abrasion, *J. Nanomater.*, 2014, **2014**, 185080.

9 N. Shandilya, O. Le Bihan and M. Morgeneyer, A Review on the Study of the Generation of (Nano)particles Aerosols during the Mechanical Solicitation of Materials, *J. Nanomater.*, 2014, **2014**, 289108.

10 F. Tou, *et al.*, Multi method approach for analysis of road dust particles: elemental ratios, SP-ICP-TOF-MS, and TEM, *Environ. Sci.: Nano*, 2022, **9**(10), 3859–3872.

11 A. Thorpe and R. M. Harrison, Sources and properties of non-exhaust particulate matter from road traffic: A review, *Sci. Total Environ.*, 2008, **400**, 270–282.

12 J. K. Gietl, R. Lawrence, A. J. Thorpe and R. M. Harrison, Identification of brake wear particles and derivation of a quantitative tracer for brake dust at a major road, *Atmos. Environ.*, 2010, **44**, 141–146.

13 P. Wåhlin, R. Berkowicz and F. Palmgren, Characterisation of traffic-generated particulate matter in Copenhagen, *Atmos. Environ.*, 2006, **40**, 2151–2159.

14 E. Apeagyei, M. S. Bank and J. D. Spengler, Distribution of heavy metals in road dust along an urban-rural gradient in Massachusetts, *Atmos. Environ.*, 2011, **45**, 2310–2323.

15 P. Pant and R. M. Harrison, Estimation of the contribution of road traffic emissions to particulate matter concentrations from field measurements: A review, *Atmos. Environ.*, 2013, **77**, 78–97.

16 K. Adachi and Y. Tainosho, Characterization of heavy metal particles embedded in tire dust, *Environ. Int.*, 2004, **30**, 1009–1017.

17 J. Wang, *et al.*, Detection and quantification of engineered particles in urban runoff, *Chemosphere*, 2020, **248**, 126070.

18 USGS, *Characterization of Stormwater Runoff from Bridges in North Carolina and the Effects of Bridge Deck Runoff on Receiving Streams*, 2011.

19 D. R. Bourcier, E. Hindin and J. C. Cook, Titanium and tungsten in highway runoff at pullman, washington, *Int. J. Environ. Stud.*, 1980, **15**, 145–149.

20 F. Loosli, *et al.*, Sewage spills are a major source of titanium dioxide engineered (nano)-particle release into the environment, *Environ. Sci.: Nano*, 2019, **6**, 763–777.

21 A. M. Saharia, Z. Zhu, N. Aich, M. Baalousha and J. F. Atkinson, Modeling the transport of titanium dioxide nanomaterials from combined sewer overflows in an urban river, *Sci. Total Environ.*, 2019, **696**, 133904.

22 M. M. Nabi, J. Wang and M. Baalousha, Episodic surges in titanium dioxide engineered particle concentrations in surface waters following rainfall events, *Chemosphere*, 2021, **263**, 128261.

23 D. L. Slomberg, *et al.*, Anthropogenic Release and Distribution of Titanium Dioxide Particles in a River Downstream of a Nanomaterial Manufacturer Industrial Site, *Front. Environ. Sci.*, 2020, 76.

24 J. Vidmar, T. Zuliani, R. Milačič and J. Ščančar, Following the Occurrence and Origin of Titanium Dioxide Nanoparticles in the Sava River by Single Particle ICP-MS, *Water*, 2022, **14**, 959.

25 N. Parker and A. A. Keller, Variation in regional risk of engineered nanoparticles: nanoTiO 2 as a case study, *Environ. Sci.: Nano*, 2019, **6**, 444–455.

26 L. N. Rand, *et al.*, Quantifying temporal and geographic variation in sunscreen and mineralogic titanium-containing nanoparticles in three recreational rivers, *Sci. Total Environ.*, 2020, **743**, 140845.

27 A. P. Gondikas, *et al.*, Release of TiO2 nanoparticles from sunscreens into surface waters: A one-year survey at the old danube recreational lake, *Environ. Sci. Technol.*, 2014, **48**, 5415–5422.

28 R. David Holbrook, *et al.*, Titanium distribution in swimming pool water is dominated by dissolved species, *Environ. Pollut.*, 2013, **181**, 68–74.

29 Y. Yang, *et al.*, Prospecting nanomaterials in aqueous environments by cloud-point extraction coupled with transmission electron microscopy, *Sci. Total Environ.*, 2017, **584–585**, 515–522.

30 A. K. Venkatesan, *et al.*, Detection and Sizing of Ti-Containing Particles in Recreational Waters Using Single Particle ICP-MS, *Bull. Environ. Contam. Toxicol.*, 2018, **100**, 120–126.

31 A. Praetorius, *et al.*, Single-particle multi-element fingerprinting (spMEF) using inductively-coupled plasma time-of-flight mass spectrometry (ICP-TOFMS) to identify engineered nanoparticles against the elevated natural background in soils, *Environ. Sci.: Nano*, 2017, **4**, 307–314.

32 H. Wang, A. S. Adeleye, Y. Huang, F. Li and A. A. Keller, Heteroaggregation of nanoparticles with biocolloids and geocolloids, *Adv. Colloid Interface Sci.*, 2015, **226**, 24–36.

33 J. Barksdale, *Titanium, Its Occurrence, Chemistry, and Technology*, Soil Science, 1950, p. 414.

34 T. Zack, A. Kronz, S. Foley and T. Rivers, Trace element abundances in rutiles from eclogites and associated garnet mica schists, *Chem. Geol.*, 2002, **184**, 97–122.

35 N. Craigie, *Principles of Elemental Chemostratigraphy*, Springer International Publishing Springer International Publishing, 2018, DOI: **10.1007/978-3-319-71216-1**.

36 J. Wang, M. M. Nabi, M. Erfani, E. Goharian and M. Baalousha, Identification and quantification of anthropogenic nanomaterials in urban rain and runoff using single particle-inductively coupled plasma-time of flight-mass spectrometry, *Environ. Sci.: Nano*, 2022, **9**, 714–729.

37 M. M. Nabi, *et al.*, Concentrations and size distribution of TiO2 and Ag engineered particles in five wastewater treatment plants in the United States, *Sci. Total Environ.*, 2021, **753**, 142017.

38 A. Praetorius, *et al.*, Single-particle multi-element fingerprinting (spMEF) using inductively-coupled plasma time-of-flight mass spectrometry (ICP-TOFMS) to identify engineered nanoparticles against the elevated natural background in soils, *Environ. Sci.: Nano*, 2017, **4**, 307–314.

39 S. Lee, *et al.*, Nanoparticle size detection limits by single particle ICP-MS for 40 elements, *Environ. Sci. Technol.*, 2014, **48**, 10291–10300.

40 M. Hadioui, *et al.*, Lowering the Size Detection Limits of Ag and TiO2 Nanoparticles by Single Particle ICP-MS, *Anal. Chem.*, 2019, **91**, 13275–13284.

41 H. E. Pace, *et al.*, Determining Transport Efficiency for the Purpose of Counting and Sizing Nanoparticles via Single Particle Inductively Coupled Plasma Mass Spectrometry, *Anal. Chem.*, 2011, **83**, 9361–9369.

42 M. Baalousha, J. Wang, M. Erfani and E. Goharian, Elemental fingerprints in natural nanomaterials determined using SP-ICP-TOF-MS and clustering analysis, *Sci. Total Environ.*, 2021, **792**, 148426.

43 A. Antignano and C. E. Manning, Rutile solubility in H2O, H2O–SiO2, and H2O–NaAlSi3O8 fluids at 0.7–2.0 GPa and 700–1000 °C: Implications for mobility of nominally insoluble elements, *Chem. Geol.*, 2008, **255**, 283–293.

44 U.S. Geological Survey, *Mineral Commodity Summaries*, 2019, DOI: **10.3133/70202434**.

45 U.S. Geological Survey (USGS), USGS Current Conditions for USGS 03451500 FRENCH BROAD RIVER AT ASHEVILLE, NC. Available at: **https://waterdata.usgs.gov/nwis/dv?cb_00045=on&format=html&site_no=03451500&referred_module=sw&period=&begin_date=2020-04-20&end_date=2020-05-10**, (Accessed: 8th January 2021).

46 City of Knoxville. Rainfall Data - City of Knoxville. Available at: **https://knoxvilletn.gov/government/city_departments_offices/engineering/stormwater_engineering_division/rainfall_data**, (Accessed: 8th January 2021).

47 U.S. Geological Survey (USGS), USGS Current Conditions for USGS 02162285 TABLE ROCK RESERVOIR NR CLEVELAND, SC. Available at: **https://waterdata.usgs.gov/nwis/dv?cb_00045=on&format=html&site_no=02162285&referred_module=sw&period=&begin_date=2020-04-27&end_date=2020-05-12**, (Accessed: 10th January 2021).

48 SCDHEC, Saluda River/Lake Murray watershed. Available at: **https://scdhec.gov/sites/default/files/docs/HomeAndEnvironment/Docs/03050109-13.pdf**, (Accessed: 16th August 2021).

49 SCE & G, S. C. Saluda Project (FERC No. 516): Lake Murray Water Quality Report.

50 National Park Service & U.S. Department of the Interior, *Assessment of Water Resources and Watershed Conditions in Congaree National Park, South Carolina*, 2010.

51 Federal Energy Regulatory Commission, *ENVIRONMENTAL ASSESSMENT FOR HYDROPOWER LICENSE*, 2020.

52 SCE & G, S. C., South Carolina Electric & Gas COL Application Part 3-Environmental Report.

53 H. Galfi, H. Österlund, J. Marsalek and M. Viklander, Mineral and Anthropogenic Indicator Inorganics in Urban Stormwater and Snowmelt Runoff: Sources and Mobility Patterns, *Water, Air, Soil Pollut.*, 2017, **228**, 1–18.

54 J. Wu, *et al.*, Metal-Containing Nanoparticles in Low-Rank Coal-Derived Fly Ash from China: Characterization and Implications toward Human Lung Toxicity, *Environ. Sci. Technol.*, 2021, **55**, 6644–6654.

55 A. Gondikas, *et al.*, Where is the nano? Analytical approaches for the detection and quantification of TiO 2 engineered nanoparticles in surface waters, *Environ. Sci.: Nano*, 2018, **5**, 313–326.

56 A. A. Markus, *et al.*, Determination of metal-based nanoparticles in the river Dommel in the Netherlands via ultrafiltration, HR-ICP-MS and SEM, *Sci. Total Environ.*, 2018, **631–632**, 485–495.

57 R. Kaegi, *et al.*, Synthetic TiO2 nanoparticle emission from exterior facades into the aquatic environment, *Environ. Pollut.*, 2008, **156**, 233–239.

58 E. Adamiec, Road environments: Impact of metals on human health in heavily congested cities of Poland, *Int. J. Environ. Res. Public Health*, 2017, **14**, 697.

59 E. Pereira, J. A. Baptista-Neto, B. J. Smith and J. J. McAllister, The contribution of heavy metal pollution derived from highway runoff to Guanabara Bay sediments - Rio de Janeiro/Brazil, *An. Acad. Bras. Cienc.*, 2007, **79**, 739–750.

60 Chemours, Ti-Pure™ Solutions for Coatings: Applications, 2018, Available at: **https://www.tipure.com/en/applications/coatings?_ga=2.22333115.1280235886.1586571265-1482119140.1586571265**, (Accessed: 10th April 2020).

61 N. Shandilya, O. Le Bihan, C. Bressot and M. Morgeneyer, Emission of titanium dioxide nanoparticles from building materials to the environment by wear and weather, *Environ. Sci. Technol.*, 2015, **49**, 2163–2170.

62 P. K. Lee, *et al.*, Lead chromate detected as a source of atmospheric Pb and Cr (VI) pollution, *Sci. Rep.*, 2016, **6**, 1–10.

63 W. Wilczyńska-Michalik, K. Rzeźnikiewicz, B. Pietras and M. Michalik, Fine and ultrafine TiO2 particles in aerosol in Kraków (Poland), *Mineralogia*, 2014, **45**, 65–77.

64 United States Geological Survey, *Mineral Commodity Summaries*, 2019, DOI: **10.3133/70202434**.

65 J. Wang, M. M. Nabi, M. Erfani, E. Goharian and M. Baalousha, Identification and quantification of anthropogenic nanomaterials in urban rain and runoff using single particle-inductively coupled plasma-time of flight-mass spectrometry, *Environ. Sci.: Nano*, 2022, **9**, 714–729.

66 P. Tian, Y. Li and Z. Yang, Effect of rainfall and antecedent dry periods on heavy metal loading of sediments on urban roads, *Front. Earth Sci. China*, 2009, **3**, 297–302.
67 Q. Yuan, H. Guerra and Y. Kim, An Investigation of the Relationships between Rainfall Conditions and Pollutant Wash-Off from the Paved Road, *Water*, 2017, **9**, 232.
68 R. B. Reed, *et al.*, Multi-day diurnal measurements of Ti-containing nanoparticle and organic sunscreen chemical release during recreational use of a natural surface water, *Environ. Sci.: Nano*, 2017, **4**, 69–77.
69 R. Kaegi, *et al.*, Release of TiO 2 – (Nano) particles from construction and demolition landfills, *NanoImpact*, 2017, **8**, 73–79.
70 M. A. Kiser, *et al.*, Titanium nanomaterial removal and release from wastewater treatment plants, *Environ. Sci. Technol.*, 2009, **43**, 6757–6763.
71 City of West Columbia City Council. West Columbia City Operated Parks Closed to Reduce Potential COVID-19 Exposure - City of West Columbia. Available at: **https://westcolumbiasc.gov/2020/03/west-columbia-city-operated-parks-closed-to-reduce-potential-covid-19-exposure/**, (Accessed: 8th January 2021).
72 City of Columbia. City of Columbia coronavirus (COVID-19) update - Stay at Home Order issued - Tuesday, March 24 at 10 a.m. Available at: **https://www.como.gov/CMS/pressreleases/view.php?id=6656**, (Accessed: 8th January 2021).
73 P. L. Verplanck, *et al.*, Evaluating the behavior of gadolinium and other rare earth elements through large metropolitan sewage treatment plants, *Environ. Sci. Technol.*, 2010, **44**, 3876–3882.